Journal of Molecular Liquids 341 (2021) 117444

Contents lists available at ScienceDirect

Journal of Molecular Liquids

journal homepage: www.elsevier.com/locate/molliq

Electrical and acoustic investigation of partial discharges in two types of nanofluids

Juraj Kurimský [a,*], Michal Rajňák [a,b,*], Miloš Šárpataky [a], Zsolt Čonka [a], Katarína Paulovičová [b]

[a] Faculty of Electrical Engineering and Informatics, Technical University of Košice, Letná 9, 04200 Košice, Slovakia
[b] Institute of Experimental Physics SAS, Watsonova 47, 04001 Košice, Slovakia

ARTICLE INFO

Article history:
Received 27 July 2021
Revised 27 August 2021
Accepted 30 August 2021
Available online 2 September 2021

Keywords:
Liquid dielectric
Partial discharge
Ferrofluids
Transformer oil
Acoustic emission
Magnetic nanoparticles

ABSTRACT

Measurements of partial discharges in liquid dielectrics are important for prediction of a serious failure of electrical equipment. Recent research findings show that application of nanoparticles in dielectric liquids may increase their resistance to partial discharges. However, physical properties of a host liquid are expected to play a decisive role in the effective suppression of partial discharges by nanoparticles. In this paper, a transformer oil prepared by a gas-to-liquid technology and a standard naphthenic transformer oil are doped with an equal amount of iron oxide nanoparticles. Determination of basic physical properties of the oils and the nanofluids is followed by an experimental investigation of partial discharges under various alternating voltage levels. The detection of partial discharges is approached by two independent methods, electrically and acoustically. Both methods revealed occurrence of partial discharges in the gas-to-liquid oil at higher voltages, as compared with the naphthenic oil. Acoustic emission energy is found one order of magnitude greater in the gas-to-liquid oil than in the naphthenic oil. The acoustic wave propagation dependence on the physical properties of the liquid is considered in the qualitative explanation of the observed phenomenon. The presence of nanoparticles can suppress partial discharges in the naphthenic oil, but not in the gas-to-liquid oil.

1. Introduction

Physical properties of traditional dielectric media have been a major limiting factor impacting the design and operation of many applications spanning from particle accelerators to electrical power systems. In the power system network, the power transformers are the crucial equipment that bridges the power generation and the transmission over a long distance. One of the key materials used nowadays in transformers for cooling and insulating purposes (filling and impregnation) is transformer oil. Mineral insulating oils extracted from crude petroleum stock have been put in this service for a long while [1]. However, recent developments in the high voltage sector and environmental regulations have put greater demands on dielectric performance and sustainability of dielectric fluids [2]. This has stimulated an intensive research on progressive dielectric fluids. Among various examples, the development of supercritical fluids [3,4] and nanofluids [5–8] exhibits a promising way to more reliable and sustainable dielectric fluids. For nanofluids in general, the majority of research is devoted to their unique thermal and heat transfer properties [9–13]. Owing to the valuable combination of both, excellent thermal and dielectric properties, the dielectric nanofluids can be considered as a new generation dielectric fluids for power and electrical engineering applications [2].

Among dielectric and insulating properties of dielectric nanofluids, dielectric permittivity and electrical breakdown field strength are the most studied quantities. It is well-known that the addition of conductive, semi-conductive or dielectric nanoparticles into a base dielectric liquid results in additional polarization processes and finally to the modification of the complex dielectric permittivity [14–17]. Numerous experimental studies have proven that the nanoparticle type, concentration, morphology and size have remarkable influence on electrical breakdown processes in dielectric nanofluids [18–21]. However, less attention has been paid to partial discharges (PD) in the nanofluids, even though PD are known as one of the main causes of transformer failures. In base transformer liquids, PD are often initiated in gas bubbles, as demonstrated experimentally and theoretically in a recent paper [22]. This initiation, particularly the PD inception voltage, may be suppressed to higher voltage levels by the presence of iron oxide nanoparticles in transformer oil [23]. Significant improvements of

* Corresponding authors at: Faculty of Electrical Engineering and Informatics, Technical University of Košice, Letná 9, 04200 Košice, Slovakia (M. Rajňák).
E-mail addresses: juraj.kurimsky@tuke.sk (J. Kurimský), rajnak@saske.sk (M. Rajňák).

https://doi.org/10.1016/j.molliq.2021.117444
0167-7322/

PD activity, including the PD inception voltage, PD amplitude and repetition rate was found for palm oil and coconut oil doped with Al_2O_3 nanoparticles [24]. TiO_2 nanoparticles dispersed in transformer oil were also found to increase the PD inception voltage and decrease the PD amplitude [25]. Another study showed positive effect of Fe_3O_4 and TiO_2 nanoparticles on the PD activity in a natural ester-based nanofluid [26]. Interestingly, not only nanoparticles as such, but also the nanoparticle interfaces and the electric double layers play an important role in the PD development in nanofluids [27].

From the literature it is seen that the research on dielectric nanofluids is directed from conventional naphthenic oil-based nanofluids to eco-friendlier alternatives, like natural ester or gas-to-liquid (GTL) oil-based nanofluids. Furthermore, most of the reported studies on PD applied one type of PD investigation method. However, even though PD in insulating materials are of the electrical nature, they are accompanied by acoustic, chemical, and optical phenomena. For this reason, various experimental methods can be used to detect PD activity [28]. The highest sensitivity of PD detection is obtained by a technique that complies with the IEC 60,270 standard, commonly called the electrical method [29]. This method allows detection of low-energy PD pulses with apparent charge lower than 0.1 pC. Nevertheless, the electrical method is not immune to electromagnetic interference and under the action of electromagnetic disturbances it can lead to false detection of PD [30]. To avoid this problem, acoustic method is often applied in practice. It is based on the fact that PD generate a transient elastic wave (acoustic emission) as a result of the rapid release of energy within the material. In addition to the detection of PD, the acoustic emission (AE) method can also localize the PD sources [31,32]. In electrical engineering, this method is used to detect PD in oil-filled power transformers [33,34] or oil-filled cables [35]. However, the PD detection sensitivity of the AE method is relatively low because only a small part of the energy of the PD current pulse is transformed into mechanical energy and also due to the AE wave attenuation. Various AE sensors have been therefore developed for a particular AE level and frequency range of ultrasonic signals [36]. In experimental research on insulating liquids, the AE sensors play a key role [37,38]. Early studies on AE generated by PD in mineral oils found that high energy (kJ) arcs radiate maximum acoustic levels in a low frequency region from 120 Hz to 10 kHz, whereas low energy (μJ) PD have maximum acoustic emission at higher frequencies from 10 kHz to 400 kHz [39].

In this work, we employ both, electrical and acoustic PD measurement methods to study PD in two different transformer oils (naphthenic and gas-to-liquid) and two nanofluids based on these oils containing the same amount of iron oxide nanoparticles. We analyze the influence of different physical properties of the two oils on the PD in the nanofluids. The PD detection by the two independent methods is compared at various voltage levels.

2. Materials and methods

2.1. Base liquids

For this study, two types of commercially available transformer insulating oils have been chosen. One is a traditional inhibited insulating oil, containing naphthenic base oils and additives that inhibit oxidation. Hereinafter, this oil is labeled as NTO (naphthenic transformer oil). The other transformer oil is a fully inhibited oil manufactured from zero Sulphur base oils produced by a gas-to-liquid (GTL) technology. We refer to this oil by GTLTO label. The basic physical parameters of the two oils are presented in Table 1 as declared by manufacturers except for the permittivity and dissipation factor. The two parameters were measured by the authors using a dielectric test set Eltel Model ADTR-2 K Plus (Eltel, IN). In addition, dynamic viscosity of the oils was measured by Physica MCR 502 rheometer (Anton Paar, AT). Concerning the color, one can observe in Fig. 1 that NTO is yellowish, while GTLTO is colorless (clear and transparent).

Table 1
Physical characteristics of the naphthenic transformer oil (NTO) and the gas-to-liquid transformer oil (GTLTO).

Properties	NTO	GTLTO
Density (kg/m^3)	865	805
Dynamic viscosity at 20 °C (mPa·s)	16.1	14.4
Flash point (°C)	155	191
Pour point (°C)	−45	−42
Dissipation factor at 20 °C	0.000498	0.000528
Permittivity at 20 °C	2.157	2.065

2.2. Nanofluids

Two nanofluids included in this study are based on the two carrier liquids, NTO and GTLTO, and hereinafter they are labeled as NNF and GTLNF, respectively. In both cases, the dispersive phase consists of superparamagnetic iron oxide nanoparticles synthesized by the chemical co-precipitation method. A single-layer of oleic acid is used as a stabilizing agent (surfactant). The visual appearance of the nanofluid samples is shown in Fig. 1. More detailed information on the nanofluid preparation has been described in our earlier papers [40–42].

In order to investigate the effect of the base liquid on the partial discharges and their acoustic emission in the nanofluids, we prepared the two nanofluids with equal nanoparticle concentrations determined by the well-known equation $c_1V_1 = c_2V_2$. The left-hand side of the equation consists of the concentration c and the sample volume V before the dilution, while the right-hand side contains the variables after the dilution. The volume concentration of the original GTLNF and NNF (before dilution) is 2.8% and 2.5%, respectively. As low nanoparticle concentrations are often capable of suppressing the partial discharges, we decided for the nanoparticle concentration of 0.001%. In Table 2, we summarize the selected characteristics of the two nanofluids.

The density values in Table 2 are found according to the classical mixing theory [43], while our measurements did not found any difference between the densities of the base oils and the nanofluids (the measurements uncertainty is 0.5 kg/m^3). The mean hydrodynamic nanoparticle diameter has been determined from the log-normal particle size distribution obtained from a dynamic light

Fig. 1. Pictures of the samples included in the study. NTO – naphthenic transformer oil, GTLTO – transformer oil prepared by the gas-to-liquid technology, NNF – nanofluid based on NTO, GTLNF – nanofluid based on GTLTO.

Table 2
Selected characteristics of the nanofluids included in this study.

Properties	NNF	GTLNF
Nanoparticle concentration (%)	0.001	0.001
Mean hydrodynamic diameter (nm)	12.2	12.2
Mean magnetic core diameter (nm)	10.3	10.3
Density (kg/m^3)	865.043	805.044
Dissipation factor at 20 °C	0.000459	0.001724
Permittivity at 20 °C	2.157	2.065

scattering (DLS) experiment (Malvern Instruments Ltd., Malvern, UK). The measurement was performed on the nanoparticles dispersed in GTLTO at room temperature (23 °C). As the two nanofluids (GTLNF and NNF) were prepared from the same batch of nanoparticle precipitate, and as the oils are practically equally non-polar, we do not expect any differences in the formation of hydrodynamic surface layers in the two oils. Therefore, the same hydrodynamic size is considered for both nanofluids. The size distribution by number is shown in Fig. 2a. The distribution of the nanoparticles' magnetic cores was derived from a magnetization curve and its fitting by a superposition of Langevin functions (Fig. 2b) [44]. The fit was performed on a magnetization of a stock concentrated GTLNF nanofluid (2.8%). The difference of the two mean diameters obtained by the different methods is ascribed to the double thickness of the surfactant and the non-magnetic layer of the nanoparticle.

The magnetization measurements were carried out by means of a vibrating sample magnetometer installed on a cryogen-free superconducting magnet from Cryogenic Limited (London, UK). In Fig. 3a, the magnetization curve of the nanoparticle powder is presented. The curve exhibits a typically high susceptibility at low magnetic field and the magnetization is well saturated at higher fields. However, when dispersed in the carrier liquids with such a low nanoparticle concentration, the positive superparamagnetic signal becomes negligible. Instead, the diamagnetic behavior of the transformer oil dominates the total magnetization of the nanofluids (Fig. 3b). From the inset in Fig. 3b, one can see just a weak positive magnetization below 0.1 T, which is overcome by the increasing diamagnetic contribution from the transformer oils with the increasing magnetic field. In the presented magnetizations, the diamagnetic contribution from the sample holder is subtracted.

2.3. Electrical detection of partial discharges

PD quantities, as introduced in the IEC 60270 standard, were acquired by MPD600 PD measurement system (Omicron Electronics, AT). The electrical connection of the experimental setup is shown in the Fig. 4. With the high potential increasing, the development of the PD apparent charge Q_{IEC} quantity (released in the C_k, DUT) was observed and recorded continuously by measuring instrument MI. The time base for the charge integration was 300 ms. After reaching the inception voltage, several potential levels, each increased by approx. 5 kV, were followed up to 60 kV. The high potential was controlled by PFT-103CM(F) AC Hipot Test Set (High Voltage Inc., USA). PD pulses, generated in the sample (DUT, C_a), were conditioned in the electronic coupling device CD, connected to a coupling capacitor C_k, and processed in the measuring instrument MI. To avoid the external electrical disturbance, the reactive filter Z was connected in series with the measuring circuit. The measured PD amount was calibrated by PD Calibrator Type 9216 (Tettex Instruments, CH).

2.4. Acoustic detection of partial discharges

The principle of the AE detection is depicted in Fig. 5. A glass beaker placed on a copper pressed profile was filled with a tested liquid. The copper profile operated as a grounded plain electrode. The high potential electrode tip curvature radius was approx.15 μm. It was immersed in the liquid. Around the tip a highly inhomogeneous electric field was formed against the grounded plain electrode. The PD discharges were released in the vicinity of the small-curvature high-potential tip surface. Unwanted mechanical acoustic bounds were damped by means of PE foam pads. The integral preamp piezoelectric sensor type RI15AST (Physical Acoustic, UK) was sensing the acoustic emission released by the PD pulses during the tests. The sensor is sensitive only in the specific frequency range satisfying low energy PD, see Fig. 6, where the gain is referenced to 1 V/1μBar. The fixed bounding with the beaker was achieved by the PE foam at the bottom and the silicone grease at the sensor contacting-sensing area on the top. The transfer of AE energy through the fluid medium was calibrated by initiating the known amount of acoustic energy by another RI15AST sensor attached to the needle, which was placed at the position of the high-potential electrode. The AE was analyzed by PCI-2 Based AE System, equipped with specific signal processor and the software (both Physical Acoustic, UK).

3. Results and discussion

The partial discharges developed in the studied liquids are presented in combined graphs consisting of a time dependent voltage applied on the electrodes and the related apparent charge Q_{IEC} and the acoustic emission (AE) detected at a particular voltage level. The apparent charge is according to IEC60270 defined as a charge that, if injected within a very short time between the terminals of the test object in a specified test circuit, would give the same reading on the measuring instrument as the PD current pulse itself. The apparent charge is usually expressed in picocoulombs (pC). One should bear in mind that the apparent charge is not equal to

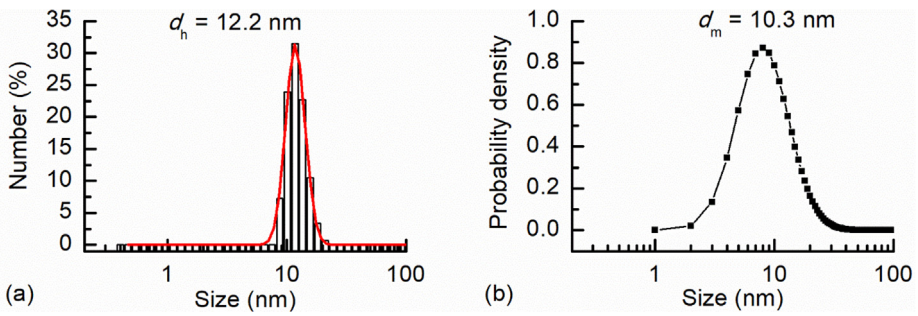

Fig. 2. (a) DLS number-based hydrodynamic particle size distribution histogram with the log-normal curve fit. (b) Log-normal distribution of nanoparticles' magnetic core size determined from magnetization measurements.

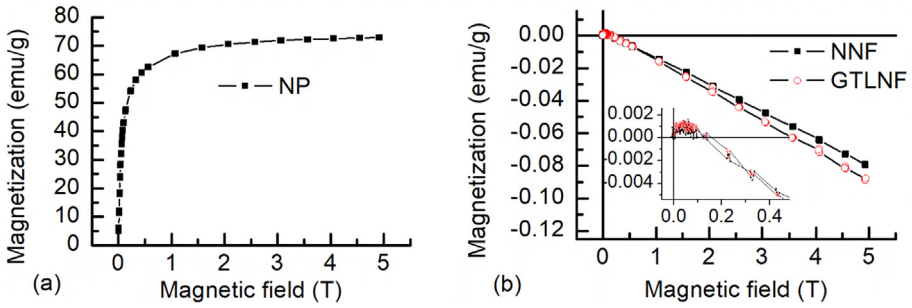

Fig. 3. Magnetization curves measured on the nanoparticle powder (a) and the nanofluids (b) at temperature of 25 °C.

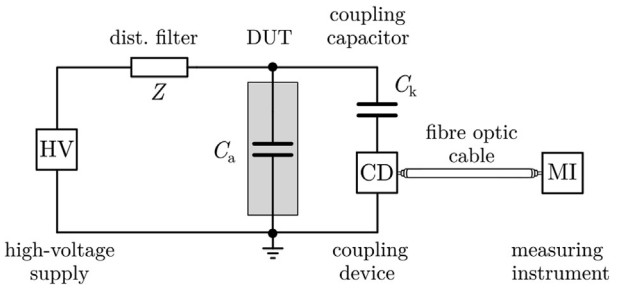

Fig. 4. Electrical connection of the experimental setup used to detect partial discharges electrically.

the amount of charge locally involved at the location of the discharge, which cannot be measured directly. The amplitude of AE signal is the highest voltage induced in the AE sensor, whereas the energy of the AE pulse is defined as the area under the AE curve or the integration of the squared voltage signal divided by the reference resistance over the total time duration of the AE pulse (the calculation derived by Physical Acoustic, UK). In Fig. 7, Q_{IEC} and the AE of partial discharges occurred in the naphthenic transformer oil (NTO) at various voltage levels are presented. From the graphs, the initial PD occurrence in NTO detected through the Q_{IEC} is observable at 35 kV voltage, when Q_{IEC} reaches approx. 0.5 nC. On the other hand, from the AE point of view, the initial PD is observable

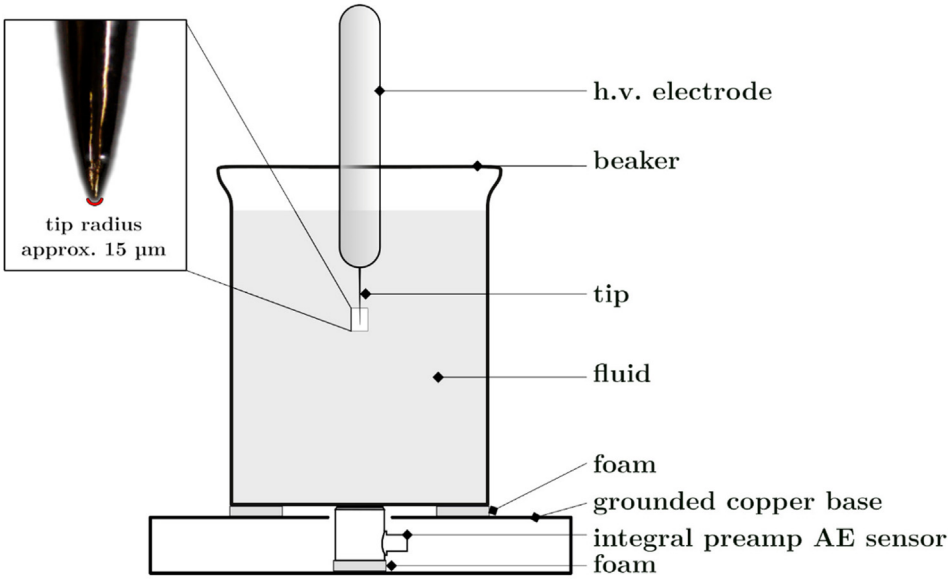

Fig. 5. Experimental setup for PD acoustic emission investigation.

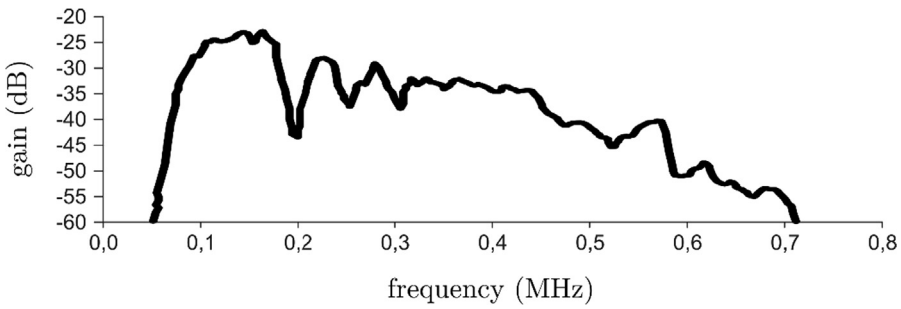

Fig. 6. AE sensor gain spectrum.

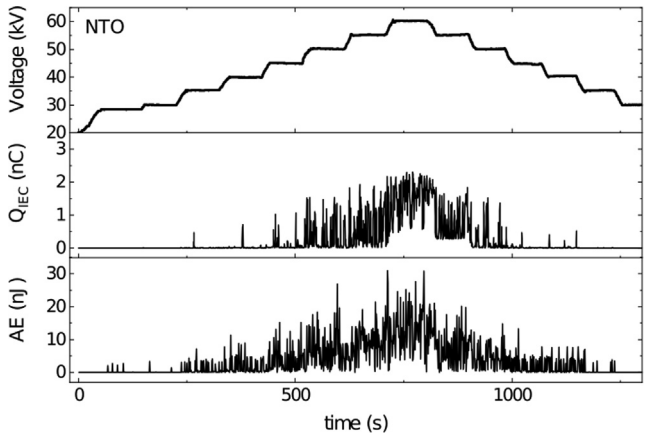

Fig. 7. Apparent charge Q_{IEC} and acoustic emission AE of partial discharges in the naphthenic transformer oil at various voltage levels.

in the particular dynamic range already at 30 kV, giving rise to the AE energy of approx. 2.5 nJ. Then, with the increasing voltage level, the PD activity intensifies, as can be seen from the increasing Q_{IEC} and AE energy. At the highest voltage applied (60 kV), the recorded Q_{IEC} and the AE in NTO are 2.2 nC and 30 nJ, respectively. By decreasing the voltage level, the extinguishing Q_{IEC} of approx. 0.5 nC is visible again at 35 kV. Based on the AE, the PD extinguish at 30 kV, with the AE energy of approx. 3 nJ. Thus, for NTO, the acoustic method reveals the initial and extinguishing PD at lower voltage than the electrical method.

In Fig. 8, Q_{IEC} and the AE recorded for the naphthenic nanofluid (NNF) is presented with respect to the applied voltage level. The voltage peak (upper graph) presents the instant of switch-on the high voltage source, when the current surge in the transformer caused a transient that was induced in the high-voltage probe. This surge, however, do not produce high voltage on the sample under test. As compared to Fig. 7, it can immediately be seen that the presence of the magnetic nanoparticles in NTO results in a significant suppression of the PD activity. This is evident from both, Q_{IEC} and the AE graphs. While for NTO the electric method revealed the initially observable PD at 35 kV with Q_{IEC} of 0.5 nC, for NNF these quantities reach 55 kV and approx. 1.5 nC – the value close to the maximal Q_{IEC} (1.8 nC). According to the electrical method, the PD in NNF easily extinguish at the voltage of 45 kV with Q_{IEC} of approx. 0.4 nC. However, the acoustic method seems to be more sensitive for observation of PD in NNF at lower voltages, as the AE energy of approx. 2 nJ can be read from the graph already from 35 kV. Similar AE energies are found for PD occurred at lower voltages (down to 30 kV) than those revealed by the electric method. The reduced PD activity in NNF is also evident from the lower AE energies, with the maximal value around 15 nJ at 60 kV.

Partial discharges released in the gas-to-liquid transformer oil (GTLTO) are presented in Fig. 9. The measurable Q_{IEC} is initially observable at the voltage of 45 kV, reaching the value 1.2 nC. Under the maximal voltage applied, the Q_{IEC} of approx. 3 nC is detected. Remarkable PD extinguish again at 45 kV with Q_{IEC} around 0.5 nC. A slightly broader voltage range causing the PD in the GTLTO is found by the acoustic method. The measurable AE starts and stops to occur at 40 kV. In comparison with PD in NTO, the PD occurrence voltage range for GTLTO is noticeably narrower. This statement is supported by both experimental methods. However, while the values of the revealed Q_{IEC} in both transformer oils are comparable, the AE energy detected in GTLTO is one order of magnitude greater than in NTO.

The effect of magnetic nanoparticles on PD in GTLTO is presented in Fig. 10. According to the electrical method, the presence of the nanoparticles in GTLTO results in moderate elimination of PD, as the Q_{IEC} exhibits slightly lower values (below 2 nC). However, the maximal AE energy in GTLNF is comparable with the one measured in GTLTO (around 250 nJ). A remarkable difference in PD in GTLTO and GTLNF is related to the voltage range in which the PD occur. As Fig. 10 shows, both, the electrical and acoustic method reveal the PD occurrence in GTLNF at lower voltage (30 kV) values than those found for GTLTO.

In addition to the above demonstrated graphs, we present the quantitative values of the partial discharge apparent charge statistically in Table 3, while the statistics related to the acoustic emission is shown in Table 4.

The presented graphs and data in the tables lead one to the following qualitative discussion. The comparison of the PD performance of the two different oils reveals that in GTLTO the PD occur in the remarkably narrower voltage range than in the NTO. This statement results from both experimental methods, revealing the initial PD occurrence in GTLTO at higher voltage than in NTO. From this point of view, the GTLTO exhibits higher resistance to PD than NTO, which may be associated with the different chemical composition of the two oils. On the other hand, the mean AE energy in GTLTO is one order of magnitude greater than the one detected in NTO (at 50 kV and 60 kV). One can further realize that the number of detected pulses in GTLTO and NTO is comparable (Table 4) and cannot be therefore a decisive parameter giving rise to the difference in the mean AE energy. The same applies to the

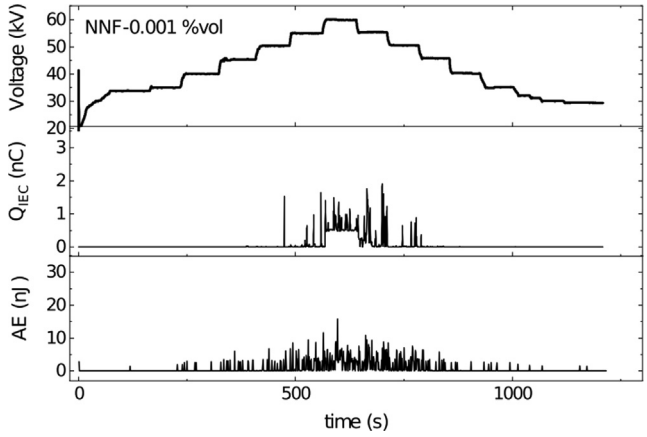

Fig. 8. Apparent charge Q_{IEC} and acoustic emission AE of partial discharges in the nanofluid based on the naphthenic transformer oil at various voltage levels.

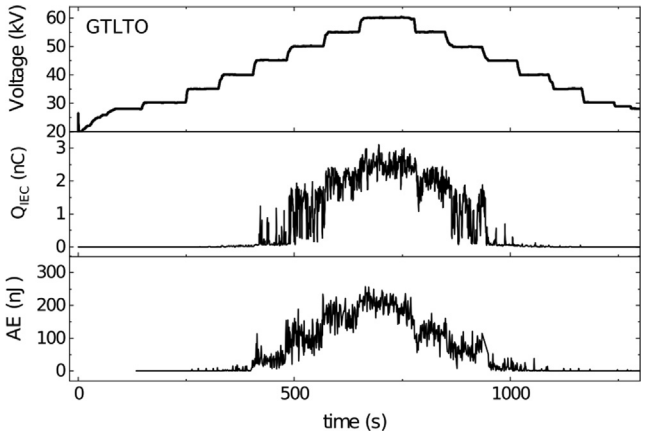

Fig. 9. Apparent charge Q_{IEC} and acoustic emission AE of partial discharges in the gas-to-liquid transformer oil at various voltage levels.

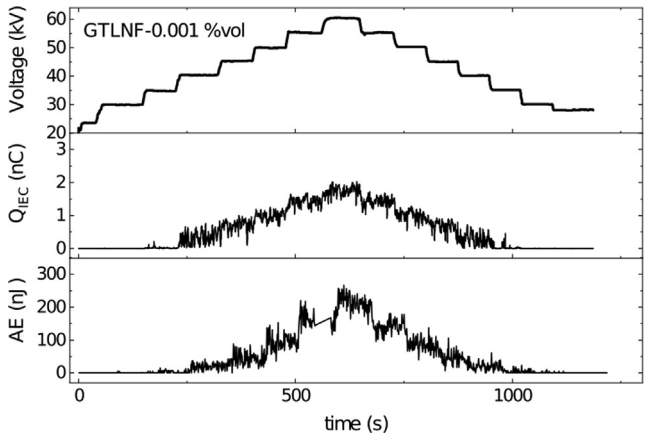

Fig. 10. Apparent charge Q_{IEC} and acoustic emission AE of partial discharges in the nanofluid based on the gas-to-liquid transformer oil at various voltage levels.

apparent charge values, which are also comparable for the two oils. Based on the definition of AE, one understands that the greater AE energy is detected via greater voltage induced in the piezoelectric sensor. It is known that the density of generated fixed charge and the resulted voltage in a piezoelectric material is proportional to the external stress acting on the sensor [45]. The stress considered in our study originates from the PD generating the transient elastic waves. The propagation of the wave towards the sensor is influenced by several factors. The first is related to the internal friction causing an eventual attenuation of the wave. As stated in Table 1, the dynamic viscosity of NTO is greater than that of GTLTO by 10.56%. This implies that in NTO the acoustic wave is attenuated in a greater measure. Subsequently, the sensor is subjected to smaller mechanical stress from the attenuated wave and that yields the determination of lower AE energy in NTO. Another possible reason of the lower AE energy detected in NTO than in GTLTO is associated with electrical polarizability of the oils. Recently, it was proven that a sound wave in a dielectric liquid propagates at a lower speed when the liquid is polarized due to an external electric field [46]. This is caused by the fact, that when a sound wave propagates through an electrically polarized medium, the polarized dipoles get closer to each other. Although the internal stresses push them away from each other, the mild electrical attraction between them delays their relaxation to a state of rarefaction. It is therefore clear that liquids which have greater dielectric permittivity get polarized to a greater extent and show a greater reduction in the speed of sound. Again, from Table 1 one can notice that the dielectric permittivity of NTO is greater by 4.27% than that of GTLTO. Thus, it can be assumed that the NTO molecules in the electric field may exhibit greater polarization than those of GTLTO. As a result, the sound wave generated by the PD may propagate at a lower speed in NTO than in GTLTO. The lower speed then results in the action of a lower mechanical stress on the sensor, when the wave transfers its kinetic energy to the sensor. This consideration

Table 3
Partial discharge apparent charge pulse statistics

Sample	Voltage level (kV)	Number of detected pulses	Mean (nC)	Standard Deviation (nC)	Minimum (nC)	Maximum (nC)
NTO	30	293	1.536E-4	9.537E-4	1.4E-12	0.0155
	40	312	0.021	0.090	4.6E-11	0.703
	50	335	0.277	0.378	0.002	1.535
	60	344	1.525	0.486	0.371	2.306
NNF	30	0	–	–	–	–
	40	177	1.220E-4	6.484E-4	3.4E-12	0.004
	50	251	0.008	0.096	4.014E-10	1.524
	60	257	0.595	0.229	1.013E-4	1.489
GTLTO	30	2	9.58E-11	0	9.58E-11	9.58E-11
	40	263	0.019	0.012	6.02E-11	0.050
	50	283	1.065	0.555	0.069	1.983
	60	422	2.481	0.243	1.688	3.104
GTLNF	30	164	2.531E-4	8.280E-4	1.5E-12	0.006
	40	322	0.310	0.196	0.005	0.760
	50	255	0.985	0.130	0.668	1.250
	60	288	1.741	0.142	1.299	2.030

Table 4
Acoustic emission response to partial discharge statistics

Sample	Voltage level (kV)	Number of detected pulses	Mean (nJ)	Standard Deviation (nJ)	Minimum (nJ)	Maximum (nJ)
NTO	30	191	0.096	0.435	3.131E-6	3.355
	40	97	1.759	2.422	3.205E-6	11.344
	50	101	6.886	5.340	0.162	26.850
	60	104	12.762	6.262	0.137	30.784
NNF	30	48	7.855E-4	0.003	3.049E-6	0.0126
	40	88	0.183	0.654	3.017E-6	2.913
	50	78	0.656	1.527	3.066E-6	6.764
	60	78	3.355	2.890	3.3491E-6	15.818
GTLTO	30	118	0.034	0.064	3.473E-6	0.474
	40	80	4.263	6.529	7.741E-6	32.870
	50	86	106.276	39.295	20.551	233.904
	60	127	200.211	27.880	97.903	256.629
GTLNF	30	103	0.180	0.800	3.850E-6	5.224
	40	97	14.396	12.111	0.0481	42.720
	50	77	72.624	34.194	13.525	152.727
	60	70	206.788	34.879	115.572	266.118

can be applied even in the case of alternating electric field of frequency of 50 Hz, because the time period of the polarization and repolarization is much longer than the time interval of the detected acoustic pulses.

From Table 3 it is seen that the presence of magnetic nanoparticles in NNF results in remarkably lower numbers of pulses detected at a particular voltage level, as compared with the number of pulses in NTO. Moreover, the mean apparent charge is also lower for NNF than for NTO. The suppressed PD activity in NNF due to the nanoparticles is confirmed by the acoustic method too, as the remarkable lower numbers of detected pulses and lower mean AE energies are also seen from Table 4. These experimental results support the earlier research findings pointing out the enhanced dielectric performance of transformer oils due to the presence of magnetic nanoparticles [23,24,26,47]. However, this enhancement cannot be convincingly alleged in the case of GTLNF. According to Table 3, the number of detected pulses in GTLNF is found lower than the number of pulses in GTLTO only at 60 kV. At lower voltages, the pulses occur more frequently in GTLNF than in GTLTO. From AE point of view, the difference in pulse occurrence in the two nanofluids (Table 4) is not so unambiguous. However, based on the presented PD data from both methods, one can conclude that the applied nanoparticles are capable of suppressing the PD activity in the standard NTO, but not in the GTLTO. The potential reason of the different effect of the nanoparticles in the different oils may be associated with different nanoparticle electrodynamics and assembly formation, as considered in another study [42]. Following the physical properties of the two oils, one can assume that the lower viscosity of GTLTO supports the migration of the nanoparticles toward the electric field gradient. There, near the electrode surface, the nanoparticles may form strong inhomogeneities in the form of assembled chains. In principle, this assembling is more facilitated in GTLNF than in NNF because of greater dielectric contrast between the nanoparticles and GTLTO, as GTLTO has slightly lower dielectric permittivity than NTO. Therefore, the nanoparticles dispersed in GTLTO may acquire greater induced electric dipoles than those dispersed in NTO. As a result, the polarized nanoparticles and their assemblies can be directed to the electrode surface. In this way, the created near-electrode inhomogeneities may increase the local field intensity, which is necessary for the initiation of the discharge.

4. Conclusion

In summary, two nanofluids with equal amount of magnetic nanoparticles dispersed in two different transformer oils were subjected to the experimental investigation of partial discharges. The problem has been approached from two perspectives, applying the electrical and acoustic method. It is found that partial discharges in the gas-to-liquid oil start to occur at higher voltage, as compared with the naphthenic oil. This is obvious from both experimental methods. However, the mean acoustic emission energy associated with partial discharges in the gas-to-liquid oil is one order of magnitude greater than the one detected in the naphthenic oil. This difference is ascribed to the different viscosity and dielectric permittivity of the two oils. The greater viscosity of the naphthenic oil causes the attenuation of the acoustic wave in a greater measure than in the gas-to-liquid oil. Subsequently, the lower acoustic emission energy is determined from the sensor subjected to the smaller mechanical stress from the attenuated wave. Another reason of the lower acoustic emission energy in the naphthenic oil is ascribed to the slightly greater dielectric permittivity of the naphthenic oil, which gives rise to greater polarization of its molecules in the electric field. As a result, the sound wave propagates at a lower speed in the naphthenic oil than in the gas-to-liquid oil and causes a lower mechanical stress on the sensor. From this point of view, the acoustic method is proven to be a very suitable complementary method for detection of partial discharges in gas-to-liquid oil. The results further showed that the magnetic nanoparticles can suppress the partial discharge activity in the standard naphthenic oil, but not in the gas-to-liquid oil. The reason of this behavior is again ascribed to the lower viscosity and dielectric permittivity of the gas-to-liquid oil, which enable more effective inhomogeneity formation in the gas-to-liquid oil than in the naphthenic oil.

Declaration of Competing Interest

The authors declare that they have no known competing financial interests or personal relationships that could have appeared to influence the work reported in this paper.

Acknowledgment

This research was funded by the Slovak Academy of Sciences and Ministry of Education in the framework of project VEGA 2/0011/20, 1/0154/21, Slovak Research and Development Agency under the contract No. APVV-18-0160, APVV-15-0438.

References

[1] R. Bartnikas, ASTM International, Electrical insulating liquids, ASTM, 1994.
[2] I. Fofana, ed., Engineering Dielectric Liquid Applications, Energies, MDPI, Basel, 2018. https://doi.org/10.3390/books978-3-03897-403-1.
[3] J. Wei, A. Cruz, F. Haque, C. Park, L. Graber, Investigation of the dielectric strength of supercritical carbon dioxide–trifluoroiodomethane fluid mixtures, Phys. Fluids. 32 (10) (2020) 103309, https://doi.org/10.1063/5.0024384.
[4] J. Wei, C. Park, L. Graber, Breakdown characteristics of carbon dioxide–ethane azeotropic mixtures near the critical point, Phys. Fluids. 32 (5) (2020) 053305, https://doi.org/10.1063/5.0004030.
[5] F. Ahmad, A.A. Khan, Q. Khan, MD.R. Hussain, State-of-Art in Nano-Based Dielectric Oil: A Review, IEEE Access. 7 (2019) 13396–13410, https://doi.org/10.1109/Access.628763910.1109/ACCESS.2019.2893567.
[6] M. Rafiq, M. Shafique, A. Azam, M. Ateeq, I.A. Khan, A. Hussain, Sustainable, Renewable and Environmental-Friendly Insulation Systems for High Voltages Applications, Molecules. 25 (2020) 3901, https://doi.org/10.3390/molecules25173901.
[7] J. Chen, P. Sun, W. Sima, Q. Shao, L. Ye, C. Li, A Promising Nano-Insulating-Oil for Industrial Application: Electrical Properties and Modification Mechanism, Nanomaterials. 9 (2019) 788, https://doi.org/10.3390/nano9050788.
[8] M. Rafiq, M. Shafique, A. Azam, M. Ateeq, The impacts of nanotechnology on the improvement of liquid insulation of transformers: Emerging trends and challenges, J. Mol. Liq. 302 (2020) 112482, https://doi.org/10.1016/j.molliq.2020.112482.
[9] D.D. Dixit, A. Pattamatta, Natural convection heat transfer in a cavity filled with electrically conducting nano-particle suspension in the presence of magnetic field, Phys. Fluids. 31 (2) (2019) 023302, https://doi.org/10.1063/1.5080778.
[10] B.H. Thang, P.H. Khoi, P.N. Minh, A modified model for thermal conductivity of carbon nanotube-nanofluids, Phys. Fluids. 27 (3) (2015) 032002, https://doi.org/10.1063/1.4914405.
[11] Z.H. Khan, W.A. Khan, M. Hamid, H. Liu, Finite element analysis of hybrid nanofluid flow and heat transfer in a split lid-driven square cavity with Y-shaped obstacle, Phys. Fluids. 32 (9) (2020) 093609, https://doi.org/10.1063/5.0021638.
[12] X.-w. Wang, Z.-P. Wan, Y. Tang, Thermodynamic and experimental study on heat transfer mechanism of miniature loop heat pipe with water-copper nanofluid, Phys. Fluids. 30 (2) (2018) 027102, https://doi.org/10.1063/1.5010244.
[13] B.M. Al-Srayyih, S. Gao, S.H. Hussain, Natural convection flow of a hybrid nanofluid in a square enclosure partially filled with a porous medium using a thermal non-equilibrium model, Phys. Fluids. 31 (4) (2019) 043609, https://doi.org/10.1063/1.5080671.
[14] M. Rajnak, B. Dolnik, J. Krempasky, R. Cimbala, K. Parekh, R. Upadhyay, K. Paulovicova, P. Kopcansky, M. Timko, Controllability of ferrofluids' dielectric spectrum by means of external electric forces, J. Phys. D. Appl. Phys. 54 (3) (2021) 035303, https://doi.org/10.1088/1361-6463/abbeb6.
[15] B. Chakraborty, K.Y. Raj, A.K. Pradhan, B. Chatterjee, S. Chakravorti, S. Dalai, Investigation of dielectric properties of TiO2 and Al2O3 nanofluids by frequency domain spectroscopy at different temperatures, J. Mol. Liq. 330 (2021) 115642, https://doi.org/10.1016/j.molliq.2021.115642.
[16] J. Fal, M. Wanic, G. Budzik, M. Oleksy, G. Żyła, Electrical Conductivity and Dielectric Properties of Ethylene Glycol-Based Nanofluids Containing Silicon

Oxide-Lignin Hybrid Particles, Nanomaterials. 9 (2019) 1008, https://doi.org/10.3390/nano9071008.
[17] M. Dong, J. Dai, Y. Li, J. Xie, M. Ren, Z. Dang, Insight into the dielectric response of transformer oil-based nanofluids, AIP Adv. 7 (2) (2017) 025307, https://doi.org/10.1063/1.4977481.
[18] P. Bartko, M. Rajňák, R. Cimbala, K. Paulovičová, M. Timko, P. Kopčanský, J. Kurimský, Effect of electrical polarity on dielectric breakdown in a soft magnetic fluid, J. Magn. Magn. Mater. 497 (2020) 166007, https://doi.org/10.1016/j.jmmm.2019.166007.
[19] Z. Wang, Y. Zhou, W.u. Lu, N. Peng, W. Chen, The impact of TiO 2 nanoparticle concentration levels on impulse breakdown performance of mineral oil-based nanofluids, Nanomaterials. 9 (4) (2019) 627, https://doi.org/10.3390/nano9040627.
[20] K.N. Koutras, I.A. Naxakis, A.E. Antonelou, V.P. Charalampakos, E.C. Pyrgioti, S. N. Yannopoulos, Dielectric strength and stability of natural ester oil based TiO2 nanofluids, J. Mol. Liq. 316 (2020) 113901, https://doi.org/10.1016/j.molliq.2020.113901.
[21] G.D. Peppas, V.P. Charalampakos, E.C. Pyrgioti, A. Bakandritsos, A.D. Polykrati, I.F. Gonos, A study on the Breakdown Characteristics of Natural Ester Based Nanofluids with Magnetic Iron Oxide and SiO2 Nanoparticles., in: ICHVE 2018 - 2018 IEEE Int. Conf. High Volt. Eng. Appl., Institute of Electrical and Electronics Engineers Inc., 2019. https://doi.org/10.1109/ICHVE.2018.8642042.
[22] S.M. Korobeynikov, A.G. Ovsyannikov, A.V. Ridel, D.I. Karpov, M.N. Lyutikova, Y.A. Kuznetsova, V.B. Yassinskiy, Study of partial discharges in liquids, in, J. Electrostat., Elsevier B.V. 103 (2020) 103412, https://doi.org/10.1016/j.elstat.2019.103412.
[23] J. Kurimský, M. Rajňák, R. Cimbala, J. Rajnič, M. Timko, P. Kopčanský, Effect of magnetic nanoparticles on partial discharges in transformer oil, J. Magn. Magn. Mater. 496 (2020) 165923, https://doi.org/10.1016/j.jmmm.2019.165923.
[24] N.A. Mohamad, N. Azis, J. Jasni, M.Z.A.A. Kadir, R. Yunus, Z. Yaakub, Experimental Study on the Partial Discharge Characteristics of Palm Oil and Coconut Oil Based Al2O3 Nanofluids in the Presence of Sodium Dodecyl Sulfate, Nanomaterials. 11 (2021) 786, https://doi.org/10.3390/nano11030786.
[25] K. Swati, K.S. Yadav, R. Sarathi, R. Vinu, M.G. Danikas, Understanding Corona discharge activity in titania nanoparticles dispersed in transformer oil under AC and DC voltages, IEEE Trans. Dielectr. Electr. Insul. 24 (4) (2017) 2325–2336, https://doi.org/10.1109/TDEI.2017.006529.
[26] M. Makmud, H. Illias, C. Chee, S. Dabbak, Partial Discharge in Nanofluid Insulation Material with Conductive and Semiconductive Nanoparticles, Materials (Basel). 12 (2019) 816, https://doi.org/10.3390/ma12050816.
[27] E.G. Atiya, D.-E. Mansour, M.A. Izzularab, Partial discharge development in oil-based nanofluids: Inception, propagation and time transition, IEEE Access. 8 (2020) 181028–181035, https://doi.org/10.1109/Access.628763910.1109/ACCESS.2020.3027905.
[28] M.M. Yaacob, M.A. Alsaedi, J.R. Rashed, A.M. Dakhil, S.F. Atyah, Review on partial discharge detection techniques related to high voltage power equipment using different sensors, Photonic Sensors. 4 (4) (2014) 325–337, https://doi.org/10.1007/s13320-014-0146-7.
[29] S.M. Hoek, S. Coenen, M. Bornowski, S. Tenbohlen, Fundamental differences of the PD measurement according to IEC 60270 and in UHF range, in: Proc. 2008 Int. Conf. Cond. Monit. Diagnosis, C. 2008, IEEE Computer Society, 2008: pp. 79–81. https://doi.org/10.1109/CMD.2008.4580234.
[30] T. Zhiguo, J. Tongtong, Research on influences factors of electromagnetic interferences for partial discharge detection in substations, in: 2017 IEEE Electr. Insul. Conf. EIC 2017, Institute of Electrical and Electronics Engineers Inc., 2017: pp. 42–45. https://doi.org/10.1109/EIC.2017.8004604.
[31] P. Kundu, N.K. Kishore, A.K. Sinha, A non-iterative partial discharge source location method for transformers employing acoustic emission techniques, Appl. Acoust. 70 (11-12) (2009) 1378–1383, https://doi.org/10.1016/j.apacoust.2009.07.001.
[32] W. Sikorski, K. Siodla, H. Moranda, W. Ziomek, Location of partial discharge sources in power transformers based on advanced auscultatory technique, IEEE Trans. Dielectr. Electr. Insul. 19 (6) (2012) 1948–1956, https://doi.org/10.1109/TDEI.2012.6396952.
[33] N.A. Akashah, M.N.K.H. Rohani, A.S. Rosmi, M. Isa, N. Rosle, B. Ismail, C.L. Wooi, A review: Partial discharge detection using acoustic sensor on high voltage transformer, in, J. Phys. Conf. Ser., Institute of Physics Publishing (2020) 12004, https://doi.org/10.1088/1742-6596/1432/1/012004.
[34] F. Witos, A. Olszewska, Z. Opilski, A. Lisowska-Lis, G. Szerszeń, Application of Acoustic Emission and Thermal Imaging to Test Oil Power Transformers, Energies. 13 (2020) 5955, https://doi.org/10.3390/en13225955.
[35] Y. Wang, X. Zhang, L. Li, J. Du, J. Gao, Design of Partial Discharge Test Environment for Oil-Filled Submarine Cable Terminals and Ultrasonic Monitoring, Energies. 12 (2019) 4774, https://doi.org/10.3390/en12244774.
[36] Sikorski, Development of Acoustic Emission Sensor Optimized for Partial Discharge Monitoring in Power Transformers, Sensors. 19 (2019) 1865. https://doi.org/10.3390/s19081865.
[37] T. Sakoda, T. Arita, H. Nieda, K. Ando, M. Otsub, C. Honda, Studies of elastic waves caused by corona discharges in oil, IEEE Trans. Dielectr. Electr. Insul. 6 (1999) 825–830, https://doi.org/10.1109/94.822022.
[38] T. Boczar, Identification of a specific type of PD from acoustic emission frequency spectra, IEEE Trans. Dielectr. Electr. Insul. 8 (2001) 598–606, https://doi.org/10.1109/94.946712.
[39] R.T. Harrold, ACOUSTIC EMISSION SIGNATURES OF ARCS AND SPARKS., in: Conf. Rec. IEEE Int. Symp. Electr. Insul., IEEE, 1980: pp. 184–189. https://doi.org/10.1109/icei.1980.7470905.
[40] K. Paulovičová, J. Tóthová, M. Rajňák, M. Timko, P. Kopčanský, V. Lisý, Nanofluid Based on New Generation Transformer Oil: Synthesis and Flow Properties, Acta Phys. Pol. A. 137 (2020) 908–910, https://doi.org/10.12693/APhysPolA.137.908.
[41] M. Rajnak, Z. Wu, B. Dolnik, K. Paulovicova, J. Tothova, R. Cimbala, J. Kurimský, P. Kopcansky, B. Sunden, L. Wadsö, M. Timko, Magnetic Field Effect on Thermal, Dielectric, and Viscous Properties of a Transformer Oil-Based Magnetic Nanofluid, Energies. 12 (2019) 4532, https://doi.org/10.3390/en12234532.
[42] Juraj Kurimsky, Michal Rajnak, Roman Cimbala, Katarina Paulovicova, Zbigniew Rozynek, Peter Kopcansky, Milan Timko, Electrical discharges in ferrofluids based on mineral oil and novel gas-to-liquid oil, J. Mol. Liq. 325 (2021) 115244, https://doi.org/10.1016/j.molliq.2020.115244.
[43] Naser Ali, Joao A. Teixeira, Abdulmajid Addali, A Review on Nanofluids: Fabrication, Stability, and Thermophysical Properties, J. Nanomater. 2018 (2018) 1–33, https://doi.org/10.1155/2018/6978130.
[44] Z. Rozynek, A. Józefczak, K.D. Knudsen, A. Skumiel, T. Hornowski, J.O. Fossum, M. Timko, P. Kopčanský, M. Koneracká, Structuring from nanoparticles in oil-based ferrofluids, Eur. Phys. J. E 2011 343. 34 (2011) 1–8. https://doi.org/10.1140/EPJE/I2011-11028-5.
[45] A. Arnau, D. Soares, Fundamentals of piezoelectricity, in: Piezoelectric Transducers Appl., Springer Berlin Heidelberg, 2008: pp. 1–38. https://doi.org/10.1007/978-3-540-77508-9_1.
[46] Amey S. Joshi, Sound waves in polarized fluids, Phys. Fluids. 31 (7) (2019) 076105, https://doi.org/10.1063/1.5096369.
[47] J. Kurimský, M. Rajňák, P. Bartko, K. Paulovičová, R. Cimbala, D. Medved', M. Džamová, M. Timko, P. Kopčanský, Experimental study of AC breakdown strength in ferrofluid during thermal aging, J. Magn. Magn. Mater. 465 (2018) 136–142, https://doi.org/10.1016/j.jmmm.2018.05.083.